Theoretical Simulations of Clamping Levels in Optical Power Limiting

Alexander Baev

Institute for Lasers, Photonics and Biophotonics, SUNY at Buffalo, Buffalo, New York 14260

Patrick Norman* and Johan Henriksson

Department of Physics, Chemistry and Biology, Linköping University, SE-581 83 Linköping, Sweden

Hans Ågren

Theoretical Chemistry, Royal Institute of Technology, SE-100 44 Stockholm, Sweden

Received: July 3, 2006; In Final Form: August 22, 2006

Multiphysics modeling, combining quantum mechanical and classical wave mechanical theories, of clamping levels has been performed for a platinum(II) organic compound in a sol−gel glass matrix. A clamping level of 2.5 μJ is found for a pulse duration of 10 ns. The excited-state absorption in the triplet manifold is shown to be crucial for clamping to occur.

I. Introduction

Laser light propagation through an optically active medium can favorably be analyzed by means of multiphysics modeling that involves an interplay of quantum mechanical and classical electromagnetic theories. In the present work we exploit this notion and address optical power limiting (OPL), induced by randomly oriented molecular materials, by combining first principles quantum mechanical calculations of molecular properties with time-domain solutions of the Maxwell equations. We demonstrate our modeling approach on π-conjugated platinum(II) acetylide that in recent experimental work has been shown to function as a broadband limiter.[1] The power limiting capability is explained in terms of a Jablonski diagram,[2] several key parameters of which previously have been determined for related platinum(II) organic compounds by use of first principle methods[3,4] and in a more general context by experiment.[5−7] In the present work we significantly widen the scope for the theoretical simulations of OPL by also including quantum mechanical simulations of excited-state properties both in the singlet and in the triplet manifold of states and by combining the molecular property calculations with a light propagation model[8,9] to retrieve estimates of the final property of interest, namely, the clamping level of the material. If successful, such a development is expected to have a large impact on the possibility to design molecular materials for OPL applications by theoretical simulations. The basic principle is that knowledge of the intrinsic molecular properties must be combined with classical pulse propagation to address the strong dependence of clamping levels on the laser pulse characteristics, such as intensity, shape, and duration time.

II. Methodology

We demonstrate the use of our simulation approach by studying the clamping levels for platinum(II) acetylide with thiophene units in the ligands under different lasing conditions. We consider the linear and nonlinear interactions between an ensemble of randomly oriented chromophores with number density N and an optical electric field. The field is phase coherent in the xy-plane (i.e., a plane wave) and propagates in the z-direction through a glass medium doped with chromophores and with thickness d according to

$$\mathbf{E}(\mathbf{r},t) = \mathcal{E}(\mathbf{r},t)\, e^{i(kz+\omega t)} + \text{c.c.} \tag{1}$$

where $k = 2\pi n/\lambda$ is the wavenumber (n is the refractive index) of the laser field and $\mathcal{E}$ is the amplitude function that corresponds to an intensity $I = c\epsilon_0|\mathcal{E}|^2/2$. The incident laser pulse is, at time $t = 0$, assumed to have a Gaussian profile characterized by its peak power and a given full width at half-maximum (fwhm) in the time domain, and with the amplitude function $\mathcal{E}(\mathbf{r},t)$, at time $t > 0$ during the propagation through the medium, determined from the paraxial wave equation[10]

$$\left(\frac{\partial}{\partial z} + \frac{1}{c}\frac{\partial}{\partial t} - \frac{i}{2k}\Delta_\perp\right)\mathcal{E}(\mathbf{r},t) = \frac{ik}{\epsilon_0}\mathscr{P}(\mathbf{r},t) \tag{2}$$

where $\mathbf{P}(\mathbf{r},t) = \mathscr{P}(\mathbf{r},t)\, e^{i(kz+\omega t)} + \text{c.c.}$ is the polarization of the medium.

The polarization of the medium has two contributions, namely, the polarizations of the host $\mathscr{P}_h$ and the chromophore $\mathscr{P}_c$

$$\mathscr{P}(\mathbf{r},t) = \mathscr{P}_h(\mathbf{r},t) + \mathscr{P}_c(\mathbf{r},t) \tag{3}$$

The host material can for instance be a solvent, sol−gel glass, or polymer matrix, which should be nonabsorbing at the frequency of interest. In addition, the polarization of the host is assumed to be linear so that it can be written as

$$\mathscr{P}_h(\mathbf{r},t) = \epsilon_0\chi_h^{(1)}(\omega)\, \mathcal{E}(\mathbf{r},t) \tag{4}$$

where $\chi_h^{(1)}$ is the electric linear susceptibility. The host susceptibility relates to the corresponding refractive index according to $\chi_h^{(1)} = n^2 - 1$.

The polarization of the chromophore governs the optical power limiting capabilities of the material. This polarization will obviously have nonlinear components, and macroscopic

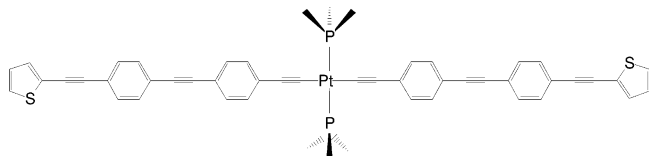* Address correspondence to this author. E-mail: panor@ifm.liu.se.

Figure 1. Molecular structure.

excited-state populations will appear during the action of the laser pulse. It is the aim of the present work to interrelate the power limiting performance and the electronic structure of the ground and excited states of the chromophore. We determine the polarization of the chromophore by use of the quantum mechanical density matrix formalism and the Liouville equation[11]

$$\frac{\partial}{\partial t}\rho_{mn} = \frac{1}{i\hbar}(H_{mk}\rho_{kn} - \rho_{mk}H_{kn}) - \gamma_{mn}(\rho_{mn} - \rho_{00}\delta_{n0}\delta_{m0}) \quad (5)$$

where the Hamiltonian matrix is a sum of the unperturbed molecular Hamiltonian (diagonal matrix with excitation energies on the diagonal) and a perturbation due to the external electric field. In the electric-dipole approximation (which applies to a given chromophore at position $\mathbf{r}_0$), the perturbation is equal to

$$\hat{V}(t) = -\hat{\mu}_\alpha E_\alpha(\mathbf{r}_0,t) \quad (6)$$

where we have introduced the electric dipole moment operator $\hat{\mu}_\alpha$ along the molecular axis α. Given the solution to eq 5, the polarization as due to the chromophore at point $\mathbf{r}_0$ is

$$\mathscr{P}_c(\mathbf{r}_0,t) = N\,\mathrm{Tr}\{\hat{\mu}\hat{\rho}\} \quad (7)$$

where N is the number density of chromophores in the medium. Our calculations account for an averaging of the molecular orientations with respect to the external electric field.

The matrix elements of the molecular Hamiltonian and the dipole moment operator as well as radiative absorption and relaxation parameters in the Liouville equation [eq 5] are determined by the use of first principles quantum chemical calculations, whereas the nonradiative relaxation parameters are set to values that are generally representative for large-sized chromophores. A detailed presentation of our methodology is found in ref 8, with underlying theory given in refs 9 and 12.

III. Computational Details

The molecular structure of the platinum(II) chromophore (ATP) is shown in Figure 1. The structure was optimized at the density functional theory (DFT) level by using the B3LYP hybrid exchange-correlation functional[13] with effective-core potentials for platinum[14] and phosphorus[15] and all-electron 6-31G[16] basis sets for the light elements. Apart from the exchange-correlation functional, an identical parametrization of the Kohn–Sham determinant was chosen for the property calculations where the time-dependent DFT (TD-DFT) approach was employed. All property calculations were performed at the ground-state optimized structure (vertical transitions), employing the Coulomb-attenuated B3LYP (CAM-B3LYP) exchange-correlation functional.[17] The geometry optimization has been performed with the Gaussian program,[18] whereas all molecular property calculations have been carried out with the Dalton program.[19]

The optimized structure of ATP belongs to the C_{2h} point group. The molecular point group of this compound is ambiguous, depending on the orientation of the phosphine and thiophene groups, see Figure 1. However, this choice is of no importance

to the optical properties of the molecules, so our choice of conformer for the theoretical work is made with respect to computational efficiency. With our choice made the molecule will be strictly planar in the optimized configuration, and due to inversion symmetry, the diagonal elements of the dipole moment matrix $\langle n|\,\hat{\mu}\,|n\rangle$ vanish. The y-axis is chosen to be the long in-plane molecular axis and the z-axis to be the out-of-plane axis. As a consequence of this choice, the components of the electric dipole operator $\hat{\mu}_x$, $\hat{\mu}_y$, and $\hat{\mu}_z$ will span the irreducible representations B_u, B_u, and A_u, respectively.

The pulse propagation simulations are performed assuming a sample thickness $d = 1$ mm and a chromophore concentration of 0.02 M. We have used fwhm values of 100 fs and 10 ns for the laser pulses, and we have considered the photon wavelengths of 532 and 694 nm. The refractive index of the medium is set to $n = 1.457$ for the two wavelengths under consideration, which corresponds to a situation where the chromophores are embedded in a sol–gel glass. In our simulations of the transmittance curves we used a 20 μm beam waist radius to estimate the pulse energy. The relaxation parameters, or inverse lifetimes, of the excited states are set to 10^6, 10^9, and 10^{12} s^{-1} for the first excited triplet state, the first excited singlet state, and other excited singlet and triplet states, respectively, and the intersystem crossing rate between the singlet and triplet manifolds is set to 10^{11} s^{-1}.

IV. Results and Discussion

A. Electronic Structure Calculations. The electronic ground state of ATP is closed-shell in nature, and therefore of singlet spin symmetry. The dominating state in the linear absorption spectrum is the 1 ^1B_u state, which to a large extent is described by a one-electron transition from the highest occupied molecular orbital of b_g symmetry to the lowest unoccupied molecular orbital of a_u symmetry. ATP is "one-dimensional" in the sense that the absorption is induced by an electric field oscillating along the molecular long in-plane y-axis—the x- and z-directed absorption can to a good approximation be ignored. This observation holds for one-photon as well as two-photon induced absorption and implies that only states of A_g symmetry are two-photon active.

As far as the quantum chemical calculations of linear and nonlinear optical properties are concerned we have chosen to adopt the density functional theory approach with the CAM-B3LYP functional. This choice is motivated by the documented good performance of this functional for response properties (including the description of charge-transfer transitions).[20,21]

The vertical electronic transition energy of the 1 ^1B_u state is predicted to be 3.39 eV (366 nm) at this level of theory, and the corresponding electric dipole transition matrix element is 8.124 au (see Table 1). In atomic units, the oscillator strength—which is proportional to the absorption strength—for the transition from the ground state S_0 to the excited state S_n is given by

$$f^{0n} = \frac{2\Delta E}{3}\sum_\alpha |M_\alpha|^2 \quad (8)$$

and for the discussed transistion to the 1 ^1B_u state the oscillator strength is as large as 5.48. This theoretical result is in good agreement with the experimental spectrum recorded in solution (tetrahydrofuran).[22] The experiment shows a highly intense and broad absorption between 350 and 420 nm that completely dominates the near-visible and visible spectrum, and the sample is accordingly slightly colored. The chromophore used in the

TABLE 1: Vertical Transition State Energies, ΔE (eV), One-Photon Moments,[a] M_α (au), and Two-photon Moments, $S_{\alpha\beta}$ (au) that Are of Predominant Importance for Optical Power Limiting at 532 and 694 nm for Molecular Compound ATP

ψ_i	ψ_f	ΔE	$|M_y|$	$|S_{yy}|$
X ^1A_g	1 ^1B_u	3.39	8.124	0
	1 ^1A_g	3.63	0	327.2
	2 ^1B_u	4.02	1.409	0
	2 ^1A_g	4.23	0	155.2
	4 ^1A_g	4.39	0	723.9
	3 ^1B_u	4.62	0.500	0
	5 ^1A_g	4.76	0	3504.4
	9 ^1A_g	5.18	0	1936.4
1 ^3B_u[b]	4 ^3A_g	1.75	0.058	0
	6 ^3A_g	2.20	0.496	0
	7 ^3A_g	2.28	0.123	0
	10 ^3A_g	2.44	2.154	0
1 ^1B_u	1 ^1A_g	0.24	1.426	0
	2 ^1A_g	0.84	0.490	0
	3 ^1A_g	0.86	0.252	0
	4 ^1A_g	1.00	2.026	0
	5 ^1A_g	1.37	9.074	0
	9 ^1A_g	1.79	2.916	0
	10 ^1A_g	2.02	0.430	0

[a] The corresponding oscillator strength is $f = 2\Delta E\sum_\alpha |M_\alpha|^2/3$. [b] The transition energy of 1 ^3B_u relative to the ground state is 1.93 eV.

experiment is that illustrated in Figure 1 but with phosphine groups that contain butyl rather than hydrogens. At the DFT/B3LYP level of theory we have determined the red-shift associated with such a change in the phosphine groups to be equal to 20 nm and we would thus expect a transition wavelength of 386 nm at the CAM-B3LYP level. A smaller red-shift is also associated with the solvent.

The conditions for our laser pulse propagation simulations will mimic those most commonly used in the experiment with respect to the laser source, that means a frequency-doubled Nd:YAG laser operating at 532 nm (2.33 eV). The laser detuning thus amounts to 31% when compared to the vertical electronic transition energy of the 1 ^1B_u state, but considering the enormous oscillator strength of the $S_0 \rightarrow S_1$ transition, the large size of the molecule, and the effects of the environment, there are several factors that will significantly broaden this absorption. The experimental linear absorption spectrum[22] shows a tail that stretches to about 550 nm. Due to this broadening, there will be an important contribution to the OPL characteristics from nonresonant linear absorption in ATP at the wavelength of the laser.

Resonant two-photon absorption (TPA) is in general believed to be of greater importance to the population of the excited states at longer wavelengths, or short pulse lengths; the reason for this assumption is that at longer wavelenths (or shorter pulse lengths) the off-resonant one-photon population of the excited states is supressed. We further assume that TPA directly followed by excited state absorption (ESA) is a relatively unlikely event. We motivate this assumption with the fact that the TP states are of gerade symmetry and above the 1 ^1B_u state in energy, and since the lifetime of the higher excited states will be short and nonradiative relaxation will occur, a macroscopic population of these states will be effectively prevented. We have therefore targeted our calculations of excited-to-excited state transition dipole moments to include only those where the 1^1B_u state acts as an initial state, see Figure 2. Furthermore, since the molecular conjugation axis is of B_u symmetry the excited-to-excited state transitions will be effective only for final states of A_g symmetry. We have determined the transition matrix elements from the 1 ^1B_u state to the 10 lowest singlet states of
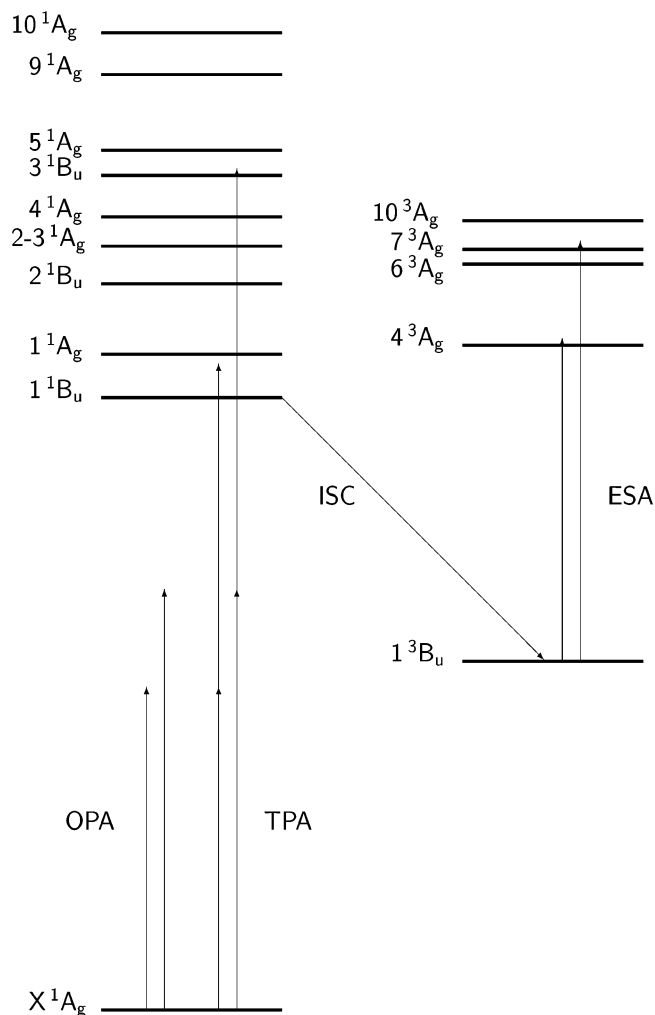

Figure 2. Electronic states of predominant importance in the simulation of the optical power limiting at 532 (2.33 eV) and 694 nm (1.79 eV) of ATP. The absorption is electric field induced whereas the relaxation processes and the intersystem crossing (ISC) are nonradiative. The figure is correctly scaled with respect to photon and transition energies; the long and short vectors correspond to photon wavelengths of 532 and 694 nm, respectively.

A_g symmetry that covers excitation energies up to 5.41 eV. The strongest absorption takes place to states 5 ^1A_g and 9 ^1A_g positioned at 4.76 and 5.18 eV, respectively, and with transition moments M_y that equal 9.07 and 2.92 au, respectively. These two states will be occupied in what we denote as a "two-step" process, which refers to nonresonant ground-to-excited states absorption followed promptly by excited-excited-state absorption (both processes having a linear dependence on the intensity of the laser field). The two individual photons involved in the two processes have a combined energy of 4.66 eV, and the two-step absorption to states 5 ^1A_g and 9 ^1A_g (via 1 ^1B_u) therefore contributes strongly to the optical power limiting performance of the material.

The population of the triplet manifold of states is important in optical power limiting applications since it causes a situation where the molecules are spin-trapped for times that are comparable to, or longer than, the duration of the laser pulse. It has been shown in experiment that the nonradiative intersystem crossing in platinum(II) organic materials is both fast and effective,[1] and it will be the predominant channel to populate the triplet manifold in our setup. Fast vibronic relaxation leads us to consider excited-to-excited-state transitions in the triplet manifold from the lowest triplet state only, i.e., the 1 ^3B_u state

Clamping Levels in Optical Power Limiting

J. Phys. Chem. B, Vol. 110, No. 42, 2006 **20915**

at 1.93 eV. We include the 10 lowest triplet states of A_g symmetry and thereby cover excitation energies up to 4.37 eV. The most important transitions within the triplet manifold are those from $1\ ^3B_u$ to states $4\ ^3A_g$ and $10\ ^3A_g$ for photon wavelengths of 694 and 532 nm, respectively. It is only in the latter case, however, that the transition moment M_y is significant (2.154 au) and the triplet state ESA should therefore be less effective at the longer of the two wavelengths. This summarizes the transitions that will govern the pulse propagation through the material. We have covered the energy region that includes nonresonant one-photon absorption and coherent two-photon absorption from the ground state and resonant excited-to-excited state one-photon transitions. We argue that the size of transition moments between a low-lying and a high-lying excited state is likely to be small due to the large number of nodes in the wave functions of the latter, which implies that the use of very extended conjugated systems may be prohibitive for the excited-to-excited-state absorption in the desired energy region, since the larger system will have a larger density of valence-excited states.

B. Pulse Propagation Calculations. The simulations of the propagation of a laser pulse through the optical power limiting material are carried out through a time integration of the combined quantum mechanical and electrodynamical equations presented in Section II. The populations of the ground and excited states of the chromophore will vary considerably during the extent of the pulse and the chromophore state propagation can therefore not be described by perturbation theory in this situation.

In a perturbational approach the coherent one- and two-photon absorption moments can be identified from the first- and second-order corrections to the expansion coefficients of the reference state in terms of the eigenstates to the zeroth-order Hamiltonian, and the corresponding one- and two-photon absorption cross sections are obtained by taking the absolute square of the moments. See for instance the book chapter by Norman and Ruud[23] for a detailed description of the perturbational approach and its application to response theory. In the past, we, and others, have made frequent use of an identification of the one- and two-photon matrix elements from the first-order residue of the linear and quadratic response functions, respectively, and it is also this approach that is used to determine the transition moments in Table 1. The one- and two-photon transition moments (M_α and $S_{\alpha\beta}$) are to be squared to obtain the corresponding absorption cross sections.

In the direct dynamical approach that is used to describe the pulse propagation in the present work there is not, and cannot be, a distinct separation between one-photon, two-photon, etc. absorption due to a mixture of excitations in the ground state and the excited state manifold. What can be clearly defined, however, are the terms in the total absorption cross section which depend linearly and nonlinearly on the intensity of the external electric field; the first two terms are typically denoted by $\sigma^{(1)}$ and $\sigma^{(2)}$. It is in the limit of short laser pulses that we can compare the absorption cross sections obtained in the perturbational approach with those obtained in the direct dynamical approach, since the short pulse will have only a small effect on the reference state. In other words, the ground-state two-photon matrix elements $S_{\alpha\beta}$ are relevant in the sense that they may describe the onset for population of the excited states by coherent multiphoton absorption, but they cannot provide the complete picture for longer pulses.

The results from simulations of the laser pulse propagation are presented in Figures 3 and 4 for the cases of short (100 fs)
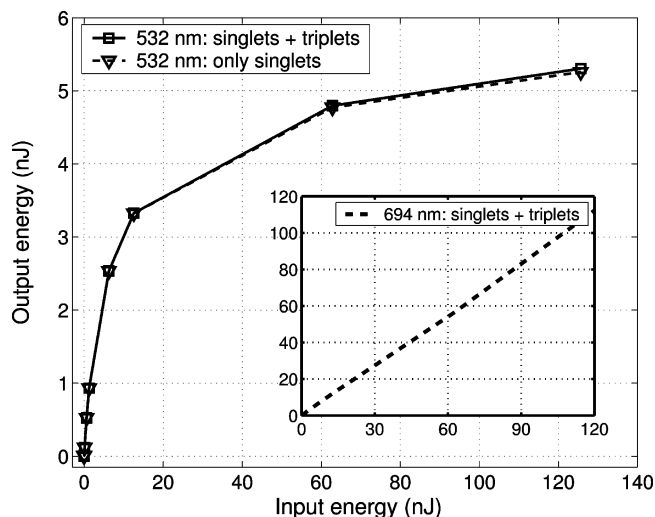
Figure 3. Optical power limiting at 532 nm with use of the ATP chromophore in a 1 mm glass at a concentration of 0.02 M. The pulse length is 100 fs.
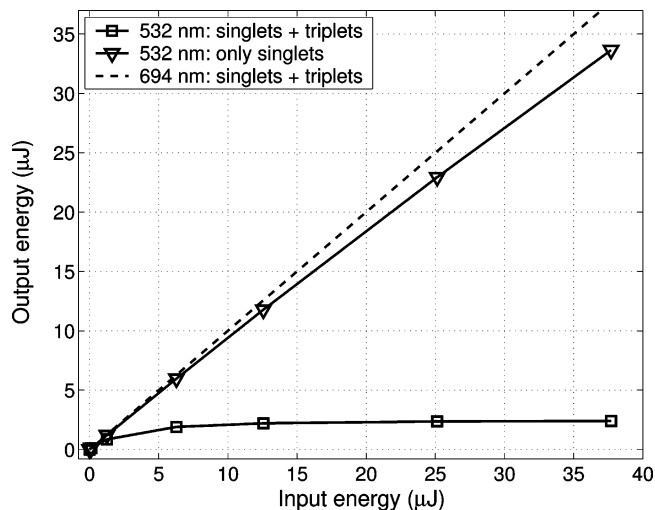
Figure 4. Optical power limiting at 532 nm with use of the ATP chromophore in a 1 mm glass at a concentration of 0.02 M. The pulse length is 10 ns.

and long (10 ns) pulses, respectively. Two separate wavelengths of 532 and 694 nm are considered, and the relative energies of the incident light versus the electronic state separations are illustrated in Figure 2.

The intersystem crossing rate is slower than the duration of the shorter pulse. In the 100 fs simulation the influence of the excited-state absorption in the triplet manifold is found negligible. An observed clamping level of about 6 nJ is found at a laser wavelength of 532 nm, regardless of whether the triplet−triplet channels are included in the simulations. For the longer wavelength the nonresonant one-photon absorption in the ground state is of course weaker than that for the short wavelength, and in addition, the two-photon resonance corresponding to state $5\ ^1A_g$ is an order of magnitude stronger than that for state $1\ ^1A_g$, which further promotes a lower clamping level at 532 nm compared to the situation at 694 nm. The inset in Figure 3 also shows that clamping is not observed at 694 nm for the laser pulse energies under consideration.

The intersystem crossing rate is, on the other hand, faster than the duration of the longer pulse, and we expect therefore that the influence of the triplet manifold increases. Our simulations clearly demonstrate that this assumption is correct;

Baev et al.

in Figure 4 it is seen that a clamping level of about 2.5 μJ is found when triplet−triplet absorption is included whereas, as triplet−triplet absorption is excluded, clamping is not reached within the energy region under consideration. This strong dependence of the optical power limiting characteristics at 532 nm on the absorption in the triplet manifold is explained by the large transition moment ($M_y = 2.154$ au) between states $1\ ^3B_u$ and $10\ ^3A_g$ (see Table 1). For the longer wavelength, on the other hand, there is no state for which the excited triplet state absorption is strong, and in the pulse propagation simulation in Figure 4 it is also seen that the absorption is virtually linear throughout the energy region of 0−40 μJ.

If we compare the results for the two pulse lengths, it is clear that the inclusion of the triplet manifold is crucial for clamping to occur with the longer of the two laser pulses but not with the shorter one. This is a result that we could not have anticipated from merely looking at the quantum mechanical results for the transition moments and excitation energies but rather it requires the consideration of the population dynamics in the chromophore medium. The reason for the requirement of the triplet manifold to obtain low-level clamping for the longer pulse is that, in this case, the excited singlet state absorption is effectively prohibited due to saturation of the high-lying singlet state. So we conclude that efficient optical power limiting relies not only on strong absorption between excited-to-excited states but also that saturation of available absorption channels (in the singlet and triplet manifolds) does not occur.

V. Concluding Remarks

We have demonstrated simulations of clamping levels in optical power limiting applications that, apart from relaxation parameters, are based on first principles. Our multiphysics modeling approach combines quantum mechanical and classical wave mechanical calculations that make it possible to pinpoint the importance of specific absorption channels to the clamping level, and that can tie the electronic structure of the chromophore to the overall performance of the material. We believe that our modeling approach provides a versatile tool to guide synthetic work.

References and Notes

(1) McKay, T. J.; Bolger, J. A.; Staromlynska, J.; Davy, J. R. *J. Chem. Phys.* **1998**, *118*, 5537.

(2) Parker, C. A. *Photoluminescence of solutions*; Elsevier: New York, 1968.

(3) Cooper, T. M.; McLean, D. G.; Rogers, J. E. *Chem. Phys. Lett.* **2001**, *349*, 31.

(4) Norman, P.; Cronstrand, P.; Ericsson, J. *Chem. Phys.* **2002**, *285*, 207.

(5) Rogers, J. E.; Cooper, T. M.; Fleitz, P. A.; Glass, D. J.; McLean, D. G. *J. Phys. Chem. A* **2002**, *106*, 10108.

(6) Rogers, J. E.; Nguyen, K. A.; Hufnagle, D. C.; McLean, D. G.; Su, W.; Gossett, K. M.; Burke, A. R.; Vinogradov, S. A.; Pachter, R.; Fleitz, P. A. *J. Phys. Chem. A* **2003**, *107*, 11331.

(7) Rogers, J. E.; Slagle, J. E.; McLean, D. G.; Sutherland, R. L.; Sankaran, B.; Kannan, R.; Tan, L.-S.; Fleitz, P. A. *J. Phys. Chem. A* **2004**, *108*, 5514.

(8) Baev, A.; Gel'mukhanov, F.; Kimberg, V.; Ågren, H. *J. Phys. B: At. Mol. Opt. Phys.* **2003**, *36*, 3761.

(9) Baev, A.; Gel'mukhanov, F.; Macak, P.; Ågren, H.; Luo, Y. *J. Chem. Phys.* **2002**, *117*, 6214.

(10) Jackson, J. D. *Classical Electrodynamics*, 3rd ed.; Wiley: New York, 1999.

(11) Boyd, R. W. *Nonlinear Optics*; Academic Press: San Diego, CA, 1992.

(12) Gel'mukhanov, F.; Baev, A.; Macak, P.; Luo, Y.; Ågren, H. *J. Opt. Soc. Am. B* **2002**, *19*, 937.

(13) Becke, A. D. *J. Chem. Phys.* **1993**, *98*, 5648.

(14) Bergner, A.; Dolg, M.; Kuchle, W.; Stoll, H.; Preuss, H. *Mol. Phys.* **1993**, *80*, 1431.

(15) Andrae, D.; Haussermann, U.; Dolg, M.; Stoll, H.; Preuss, H. *Theor. Chim. Acta* **1990**, *77*, 123.

(16) Hehre, W. J.; Ditchfield, R.; Pople, J. A. *J. Chem. Phys.* **1972**, *56*, 2257.

(17) Yanai, T.; Tew, D. P.; Handy, N. C. *Chem. Phys. Lett.* **2004**, *393*, 51.

(18) Frisch, M. J.; Trucks, G. W.; Schlegel, H. B.; Scuseria, G. E.; Robb, M. A.; Cheeseman, J. R.; Zakrzewski, V. G.; Montgomery, J. A., Jr.; Stratmann, R. E.; Burant, J. C.; Dapprich, S.; Millam, J. M.; Daniels, A. D.; Kudin, K. N.; Strain, M. C.; Farkas, O.; Tomasi, J.; Barone, V.; Cossi, M.; Cammi, R.; Mennucci, B.; Pomelli, C.; Adamo, C.; Clifford, S.; Ochterski, J.; Petersson, G. A.; Ayala, P. Y.; Cui, Q.; Morokuma, K.; Malick, D. K.; Rabuck, A. D.; Raghavachari, K.; Foresman, J. B.; Cioslowski, J.; Ortiz, J. V.; Stefanov, B. B.; Liu, G.; Liashenko, A.; Piskorz, P.; Komaromi, I.; Gomperts, R.; Martin, R. L.; Fox, D. J.; Keith, T.; Al-Laham, M. A.; Peng, C. Y.; Nanayakkara, A.; Gonzalez, C.; Challacombe, M.; Gill, P. M. W.; Johnson, B.; Chen, W.; Wong, M. W.; Andres, J. L.; Gonzalez, C.; Head-Gordon, M.; Replogle, E. S.; Pople, J. A. *Gaussian 98*; Gaussian, Inc.: Pittsburgh, PA, 1998.

(19) Dalton, a molecular electronic structure program, release 2.0, 2005.

(20) Peach, M. J. G.; Helgaker, T.; Salek, P.; Keal, T. W.; Lutnæs, O. B.; Tozer, D. J.; Handy, N. C. *Phys. Chem. Chem. Phys.* **2006**, *8*, 558.

(21) Paterson, M. J.; Christiansen, O.; Pawlowski, F.; Jørgensen, P.; Hättig, C.; Helgaker, T.; Salek, P. *J. Chem. Phys.* **2006**, *124*, 054322.

(22) Lopes, C. Private communication.

(23) Norman, P.; Ruud, K. In *Nonlinear optical properties of matter: From molecules to condensed phases*; Papadopoulos, M., Leszczynski, J., Sadlej, A. J., Eds.; Kluwer Academic Press: New York, 2006.